Ground states of the generalized Falicov-Kimball model in one and two dimensions

P. Farkašovský[a] and H. Čenčariková

Institute of Experimental Physics, Slovak Academy of Sciences Watsonova 47, 043 53 Košice, Slovakia

Abstract. A combination of small-cluster exact-diagonalization calculations and a well-controlled approximative method is used to study the ground-state phase diagram of the spin-one-half Falicov-Kimball model extended by the spin-dependent on-site interaction between localized (f) and itinerant (d) electrons. Both the magnetic and charge ordering are analysed as functions of the spin-dependent on-site interaction (J) and the total number of itinerant (N_d) and localized (N_f) electrons at selected U (the spin-independent interaction between the f and d electrons). It is shown that the spin-dependent interaction (for $N_f = L$, where L is the number of lattice sites) stabilizes the fully polarized (FP) and partially polarized (PP) state, while the stability region of the non polarized (NP) phase is gradually reduced. The precisely opposite effect on the stability of FP, PP and NP phases has a reduction of N_f. Moreover, the strong coupling between the f and d-electron subsystems is found for both $N_f = L$ as well as $N_f < L$.

PACS. 75.10.Lp Band and itinerant models – 71.27.+a Strongly correlated electron systems; heavy fermions – 71.28.+d Narrow-band systems; intermediate-valence solids 71.30.+h Metal-insulator transitions and other electronic transitions

1 Introduction

In the past decade, a considerable amount of effort has been devoted to understand the underlying physics that leads to a charge ordering in strongly correlated electron systems. The motivation was clearly due to the observation of a such ordering in doped nickelate [1] and cuprate [2] materials, some of which constitute materials that exhibit high-temperature superconductivity. One of the simplest models suitable to describe charge ordered phases in interacting electron systems is the Falicov-Kimball model (FKM) [3]. Indeed, it was shown that already the simplest version of this model (the spinless FKM) exhibits an extremely rich spectrum of charge ordered solutions, including various types of periodic, phase-separated and striped phases [4]. However, the spinless version of the FKM, although non-trivial, is not able to account for all aspects of real experiments. For example, many experiments show that a charge superstructure is accompanied by a magnetic superstructure [1,2]. In order to describe both types of ordering in the unified picture Lemanski [5] proposed a simple model based on a generalization of the spin-one-half FKM with an anisotropic, spin-dependent local interaction that couples the localized and itinerant subsystems. The model Hamiltonian is

$$H = \sum_{ij\sigma} t_{ij} d_{i\sigma}^+ d_{j\sigma} + U \sum_{i\sigma\sigma'} f_{i\sigma}^+ f_{i\sigma} d_{i\sigma'}^+ d_{i\sigma'}$$
$$+ J \sum_{i\sigma} (f_{i-\sigma}^+ f_{i-\sigma} - f_{i\sigma}^+ f_{i\sigma}) d_{i\sigma}^+ d_{i\sigma}, \quad (1)$$

a e-mail: farky@saske.sk

where $f_{i\sigma}^+$, $f_{i\sigma}$ are the creation and annihilation operators for an electron of spin $\sigma = \uparrow, \downarrow$ in the localized state at lattice site i and $d_{i\sigma}^+$, $d_{i\sigma}$ are the creation and annihilation operators of the itinerant electrons in the d-band Wannier state at site i.

The first term of (1) is the kinetic energy corresponding to quantum-mechanical hopping of the itinerant d electrons between sites i and j. These intersite hopping transitions are described by the matrix elements t_{ij}, which are $-t$ if i and j are the nearest neighbors and zero otherwise (in the following all parameters are measured in units of t). The second term represents the on-site Coulomb interaction between the d-band electrons with density $n_d = N_d/L = \frac{1}{L} \sum_{i\sigma} d_{i\sigma}^+ d_{i\sigma}$ and the localized f electrons with density $n_f = N_f/L = \frac{1}{L} \sum_{i\sigma} f_{i\sigma}^+ f_{i\sigma}$, where L is the number of lattice sites. The third term is the above mentioned anisotropic, spin-dependent local interaction of the Ising type between the localized and itinerant electrons that reflects the Hund's rule force. Moreover, it is assumed that the on-site Coulomb interaction between f electrons is infinite and so the double occupancy of f orbitals is forbidden.

Thus from the major interaction terms that come into account for the interacting d and f electron subsystems only the Hubbard type interaction between the spin-up and spin-down d electrons has been omitted in the Hamiltonian (1). In his work [5] Lemanski presents a simple justification for the omission of this term, based on an intuitive argument: the longer time electrons occupy the same site, the more important becomes interaction between them. According to this rule the interaction
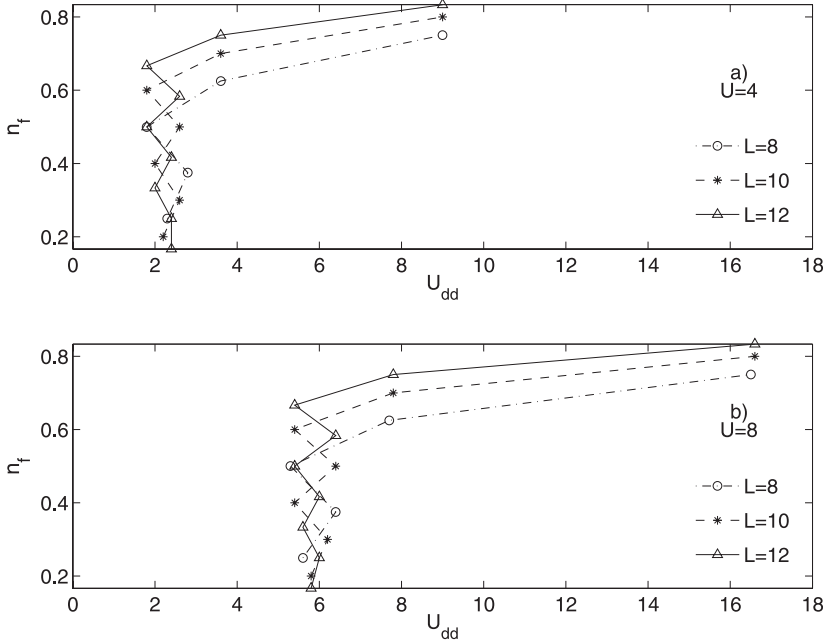
Fig. 1. The ground-state phase diagrams of the spin-one-half FKM extended by the Hubbard interaction between the itinerant electrons calculated for two different values of U on small finite clusters of $L = 8, 10$ and 12 sites. Below U_{dd}^c the ground states are the ground-state configurations of the conventional spin-one-half FKM ($U_{dd} = 0$). Above U_{dd}^c these ground states become unstable. The one-dimensional exact-diagonalization results.

between the itinerant d electrons (U_{dd}) is smaller than the interaction between the localized f electrons (U_{ff}) as well as smaller than the spin-independent interaction between the localized and itinerant electrons U. In this paper we specify more precisely conditions when this term can be neglected. For this reason we start our study with the case $U_{dd} \neq 0$. To determine the effects of U_{dd} interaction on the ground-states of the conventional spin-one-half FKM ($J = 0$) the exhaustive studies of the ground-state phase diagrams of the model (in the $n_f - U_{dd}$ plane) are performed for several cluster sizes. Of course, an inclusion of the U_{dd} term makes the Hamiltonian (1) intractable by methods used for the conventional spin-one-half/spinless FKM and thus it is necessary to use other numerical methods. Here we use the Lanczos method to study exactly the ground states of the spin-one-half FKM generalized with U_{dd} interaction between the spin-up and spin-down d electrons.

2 Results and discussion

2.1 The spin-1/2 FKM with the Hubbard interaction between itinerant electrons

The Hamiltonian of the spin-1/2 FKM with the Hubbard interaction between itinerant d electrons can be written as the sum of three terms:

$$H = \sum_{ij\sigma} t_{ij} d_{i\sigma}^+ d_{j\sigma} + U \sum_{i\sigma\sigma'} f_{i\sigma}^+ f_{i\sigma} d_{i\sigma'}^+ d_{i\sigma'}$$
$$+ U_{dd} \sum_i d_{i\uparrow}^+ d_{i\uparrow} d_{i\downarrow}^+ d_{i\downarrow}. \quad (2)$$

Since the f-electron density operators $f_{i\sigma}^+ f_{i\sigma}$ of each site i commute with the Hamiltonian (2), the f-electron occupation number is a good quantum number, taking only

two values, $w_{i\sigma} = 0, 1$ according to whether the site i is unoccupied or occupied by the localized f electron of spin σ. Therefore the Hamiltonian (2) can be rewritten as

$$H = \sum_{ij\sigma} h_{ij} d_{i\sigma}^+ d_{j\sigma} + U_{dd} \sum_i d_{i\uparrow}^+ d_{i\uparrow} d_{i\downarrow}^+ d_{i\downarrow}, \quad (3)$$

where $h_{ij} = t_{ij} + U(w_{i\downarrow} + w_{i\uparrow})\delta_{ij}$. This Hamiltonian can be considered as a generalized Hubbard model. To determine the ground-state energy of the model we have used the Lanczos method [6] and the periodic boundary conditions. However, since the hopping amplitudes depend now on the f-electron distribution $w = \{w_1, w_2 \ldots w_L\}$ (we remember that the double occupancy of f orbitals is forbidden $w_i = w_{i\uparrow} + w_{i\downarrow} = 0, 1$) the Lanczos procedure has to be used many times (strictly said $L!/((L-N_f)!N_f!)$ times) for given L and N_f. Of course, such a procedure demands in practice a considerable amount of CPU time, which imposes severe restrictions on the size of clusters that can be studied within the exact-diagonalization method. For this reason we were able to investigate exactly only the clusters up to $L = 12$. Fortunately, it was found that in some parameter regimes the ground-state characteristics of the model are practically independent of L and thus already such small clusters can be used satisfactorily to represent the behavior of macroscopic systems. In particular, we have studied the stability of the ground-state configuration $w^0(N_f)$ (obtained for $U_{dd} = 0$ and fixed N_f) at finite values of U_{dd}. The results of numerical calculations obtained for $U = 4$ and $U = 8$ are summarized in Figure 1 in the form of $n_f - U_{dd}$ phase diagrams (the half-filled band case $n_f + n_d = 1$ is considered). One can see that the ground-state configuration $w^0(N_f)$ found for $U_{dd} = 0$ persists as a ground state up to relatively large values of U_{dd} ($U_{dd}^c \sim 2$, for $U = 4$ and $U_{dd}^c \sim 6$, for $U = 8$), revealing small effects of the U_{dd} term on the ground state of the model in the strong U interaction limit. Contrary to

the strong coupling case, for small ($U = 1$) and intermediate ($U = 2$) values of the Coulomb interaction between the localized and itinerant electrons very strong effects of U_{dd} term on the ground states of the model have been observed. In these cases the typical values of U_{dd}^c are of order 0.5 but for some N_f even much smaller values were found. Thus we can conclude that the Hubbard type interaction between the spin-up and spin-down d electrons can be neglected in the strong interaction limit between the localized and itinerant electrons ($U \geq 4$). For this reason all next calculations on the spin-one-half FKM with spin-dependent Coulomb interaction J between the f and d electrons have been done at $U = 4$.

2.2 The spin-1/2 FKM with the spin-dependent interaction between itinerant and localized electrons

The spin-dependent interaction term H_J between the itinerant (d) and localized (f) electrons does not violate the condition $[f_{i\sigma}^+ f_{i\sigma}, H] = 0$ and thus the Hamiltonian (1) can be rewritten as

$$H = \sum_{ij\sigma} h_{ij} d_{i\sigma}^+ d_{j\sigma}, \qquad (4)$$

where $h_{ij} = t_{ij} + (Uw_i + Jw_{i\downarrow} - Jw_{i\uparrow})\delta_{ij}$. Thus for a given f-electron configuration $w = \{w_1, w_2 \ldots w_L\}$, the Hamiltonian (4) is the second-quantized version of the single-particle Hamiltonian $h(w)$, so the investigation of the model (4) is reduced to the investigation of the spectrum of h for different configurations of f electrons. This can be performed exactly, over the full set of f-electron distributions (including their spins), or approximatively, over the reduced set of f-electron configurations. The second way has been used in the original work by Lemanski [5]. He studied the two-dimensional version of the model using the method of restricted phase diagrams (all possible configurations of the localized f electrons for which the number of sites per unit cell is less or equal to 4 are considered) and presented some preliminary results concerning the charge and magnetic order in the ground-state of this model. For example, he detected various phases with complex charge and magnetic structures that form consecutive stages of transformation of ferromagnetic to antiferromagnetic phase with an increase of the band filling. In the present work we study the one ($D = 1$) and two ($D = 2$) dimensional analogue of the model. To determine the ground states of the model we use the method of small cluster-exact diagonalization calculations in a combination with a well-controlled numerical method [7].

Since the d electrons do not interact among themselves, the exact numerical calculations on finite clusters precede directly in the following steps: (i) Having U, J and $w = \{w_1, w_2 \ldots w_L\}$ fixed, find all eigenvalues λ_k of $h(w)$. (ii) For a given $N_f = \sum_i w_i$ and N_d determine the ground-state energy $E(w) = \sum_{k=1}^{N_d} \lambda_k$ of a particular f-electron configuration w by filling in the lowest N_d one-electron levels (the spin degeneracy must be taken into account). (iii) Find the w^0 for which $E(w)$ has a minimum. Repeating this procedure for different values of N_f, N_d, U and J, one can immediately study the ground-state phase-diagrams of the model in different parameter spaces.

To reveal an influence of the anisotropic, spin-dependent interaction between the localized and itinerant electrons on the ground states of the model we have started the study with the case $N_f = L$ ($D = 1$). In this case each lattice site is occupied by one (up or down) f electron (the double occupancy is forbidden) and thus only distributions over different spin configurations should be examined. Although the total number of configurations increases very rapidly with the cluster size L (as 2^L), relatively large lattices can be reached by this method ($L \sim 32$) if all symmetries of the Hamiltonian are considered. In Figure 2 we summarize numerical results obtained by small-cluster exact diagonalization calculations on the largest cluster that we were able to consider exactly ($L = 32$) in the form of $N_d - J$ phase diagram. To avoid an ambiguity in determination of PP and NP phases we examined the ground states only for even N_d. In the J direction the calculations have been done with step $\Delta J = 0.05$. Various phases that enter into the phase diagram are classified according to $S_f^z = \sum_i (w_{i\uparrow}^0 - w_{i\downarrow}^0)$ and $S_d^z = N_{d\uparrow} - N_{d\downarrow}$: the fully polarized (FP) phase is characterized by $|S_f^z| = N_f, |S_d^z| = N_d$, the partially polarized (PP) phases are characterized by $0 < |S_f^z| < N_f, 0 < |S_d^z| < N_d$ and the non polarized (NP) phases are characterized by $|S_f^z| = 0, |S_d^z| = 0$. Comparing numerical results obtained for $|S_f^z|$ and $|S_d^z|$ one can find a nice correspondence between the magnetic phase diagrams of localized (f) and itinerant (d) subsystems. Indeed, with the exception of several isolated points at $J = 0.05$, the corresponding FP, PP and NP phases perfectly coincide over the remaining part of diagrams showing on the strong coupling between the magnetic subsystems of localized and itinerant electrons for nonzero values of J. It is interesting that already very small changes of the spin-dependent interaction can produce so important cooperative changes. This confirms the supposition that the spin-dependent interaction between the localized and itinerant electrons could play an important role in description of ground state properties of the generalized FKM. In general, the spin-dependent interaction J stabilizes the FP and PP phases while the NP phase is gradually suppressed with increasing J. Moreover, we have observed that within the NP phase (with the exception of cases $N_d = 14, 26$) the ground states (for given N_d) do not change when J increases, while within the PP phase very strong effects of J on ground states were found (see Fig. 2). For example, the transition from the NP to FP phase at $N_d = 12$ realizes through the following sequence of PP phases: $[\uparrow_2\downarrow_6]_4 \rightarrow \uparrow_{21}\downarrow_2\uparrow_2\downarrow_3\uparrow_2\downarrow_2 \rightarrow \uparrow_{26}\downarrow_2\uparrow_2\downarrow_2 \rightarrow \uparrow_{30}\downarrow_2$, where the lower index denotes the number of consecutive sites occupied by up or down spin f electrons, or the number of repetitions of the block $[\ldots]$. In Figure 2 we present also the complete set of ground-state configurations (obtained on the above specified set of N_d and J values) from the NP region. Between them one can find different types of periodic and non-periodic configurations, but the
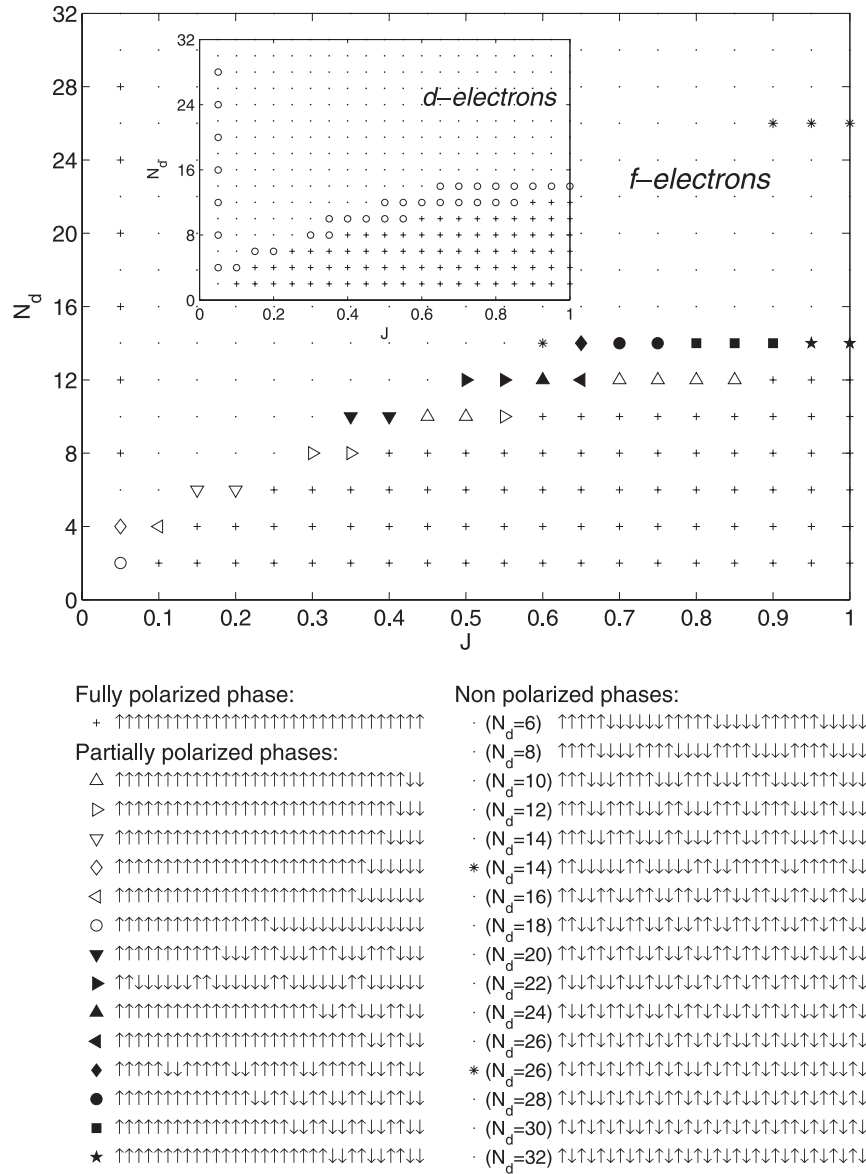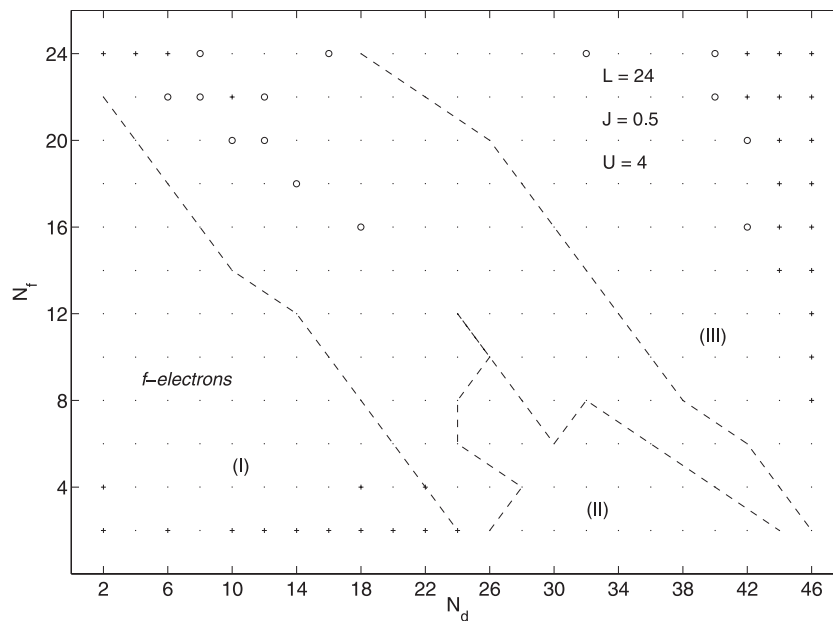
Fig. 2. The f-electron ground-state phase diagram of the spin-one-half FKM extended by the spin-dependent interaction calculated for $N_f = L$ ($L = 32$). The one-dimensional exact-diagonalization results. Inset: the d-electron ground-state phase diagram of the model calculated at the same values of model parameters. ($\cdot$): the NP phase, ($+$): the FP phase, ($\circ$): the PP phase.

most interesting examples represent configurations formed by antiparallel ferromagnetic domains, that illustrate convincingly the cooperative effects of spin-dependent interaction J between the localized and itinerant electrons.

Let us turn our attention to the case $N_f \neq L$. From the numerical point of view this case is considerably exacting, since now we have to minimize the ground state energy not only over all different spin configurations but also over all different f-electron distributions. This takes a considerable amount of CPU time and for this reason we were able to investigate exactly only the clusters up to $L = 24$ for $N_f \neq L$. In Figure 3 we present the one-dimensional skeleton phase diagram of the generalized FKM in the $N_f - N_d$ plane obtained by small-cluster exact diagonalization cal-

culations for $L = 24, U = 4$ and $J = 0.5$. Again, the stability regions of NP, FP and PP phases are marked by ($\cdot$), ($+$) and ($\circ$). Here we displayed the numerical results only for the localized subsystem since the analysis of $|S_d^z|$ and $|S_f^z|$ showed that the FP, PP, and NP phases corresponding to localized and itinerant subsystems coincide also for $N_f < L$ (similarly as for $N_f = L$, only a few exceptions have been observed in isolated points that result probably from the finite-size effects). The most striking feature of the $N_f - N_d$ phase diagram is that with decreasing N_f the NP phase is stabilized, while the FP and PP phases are suppressed. It is interesting that this effect is strongly asymmetric and a disappearance of FP and PP phases realizes in two different ways. For small d-electron concentrations the FP phase disappears practically immediately
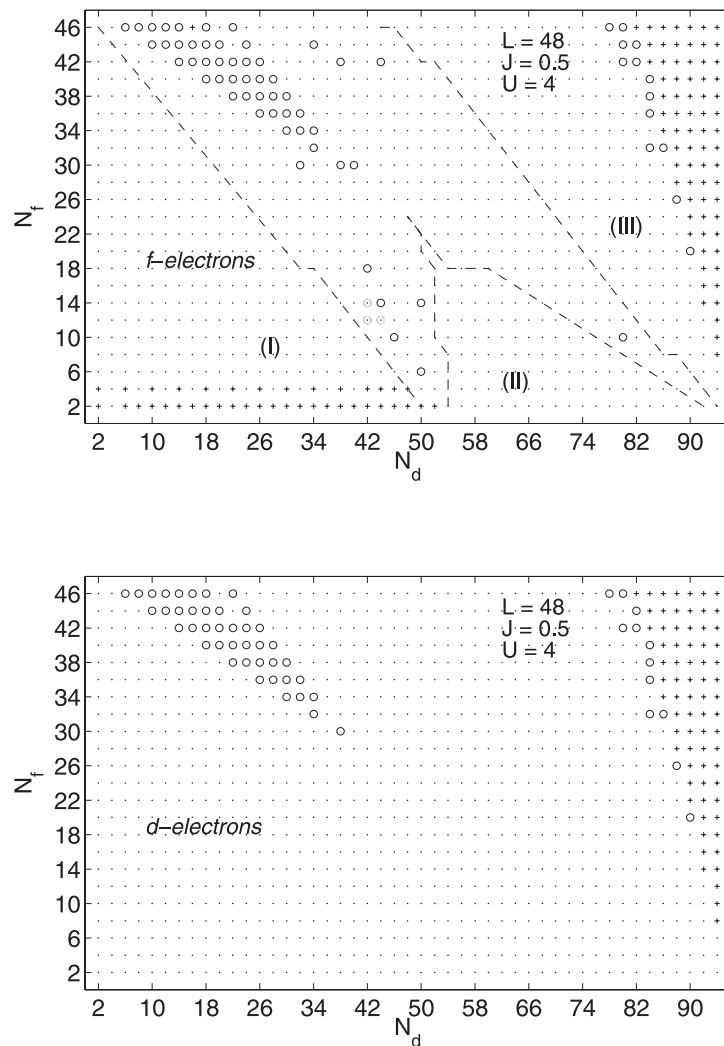
Fig. 3. The f electron skeleton phase diagram of the spin-one-half FKM extended by the spin-dependent interaction calculated for $N_f \leq L, J = 0.5$ and $L = 24$. (·): the NP phase, (+): the FP phase, (○): the PP phase. The one-dimensional exact-diagonalization results. (See the text for a definition of configuration types that are ground states in the areas I, II and III.)

outside the point $N_f = L$. The PP phase survives along the main diagonal in the narrow band and fully disappears near the point $N_f = L/2, N_d = L$. In the opposite limit (large d-electron concentrations) the FP phase persists for a wide interval of $N_f < L$ and with decreasing N_f disappears gradually. The PP phase exhibits the same behaviour. The FP phase appears also for $N_f \to 0$. However, in this limit strong finite-size effects have been observed, and thus it is questionable if this phase persists really in the thermodynamic limit.

Although the skeleton phase diagram of the generalized FKM is rather simple, the spectrum of magnetic solutions that yields the model for the NP and PP phases is very rich. Indeed, for $L = 24$ and $J = 0.5$ we have found 140 different NP phases and 20 different PP phases that enter into the $N_f - N_d$ phase diagram. Of course, it is not possible to present here all ground-state configurations, but let us show at least several main configuration types, with the largest stability regions. From the NP phases the largest stability region (denoted by I) corresponds to configurations of the type $\uparrow_n\downarrow_n 0_{L-2n}$. The second largest region (denoted by II) corresponds to NP configurations of the type $[\uparrow 0_n \downarrow 0_n]_k 0_{L-2k(n+1)}$. Typical examples of the NP ground states from the central region of the phase diagram represent periodic configurations of the type $\uparrow_n 0_m \downarrow_n 0_m$ (below the main diagonal) and configurations of the type $\uparrow_2 [\downarrow\uparrow]_{k_1} \downarrow_2 0_m[\downarrow 0_p \uparrow 0_p]_{k_2}$, or $\uparrow_2 [\downarrow\uparrow]_{k_1} \downarrow_2 0_m[\downarrow 0_p \uparrow 0_{p-1}]_{k_2}$, above the main diagonal. Between these configurations and the FP region the ground states are the segregated configurations of the type $\uparrow_2 [\downarrow\uparrow]_k \downarrow_2 0_m$, or $[\uparrow\downarrow]_{k_1} \uparrow_2 [\downarrow\uparrow]_{k_2} \downarrow_2 [\uparrow\downarrow]_{k_3} 0_m$, or their modifications (the region denoted by III). In the PP region the typical examples of ground states represent configurations of the type $\uparrow_n [0 \downarrow 0 \uparrow]_k 0 \downarrow 0$.

These results show that the spectrum of magnetic and charge solutions that yields the spin-one-half FKM model generalized with the spin-dependent interaction between the localized and itinerant electrons is indeed very rich. Of course, one can ask if these phases persist also on larger clusters. Unfortunately, lattices larger than $L = 32$ (for $N_f = L$), or $L = 24$ (for $N_f < L$) are beyond the reach of present day computers within the exact diagonalization technique. Therefore, to resolve this problem one has to use other numerical methods. Very promising seems to be the well-controlled numerical method that we have elaborated recently to study ground states of the spinless FKM [7]. This method is described in detail in our previous papers [7,8] and thus we summarize here only the main steps of the algorithm that is a simple modification of the exact-diagonalization algorithm described above: (i) Chose a trial configuration $w = \{w_1, w_2, \ldots, w_L\}$. (ii) Having w, U and J fixed, find all eigenvalues λ_k of $h(w)$. (iii) For a given $N_f = \sum_i w_i$ and N_d determine the ground-state energy $E(w) = \sum_{k=1}^{N_d} \lambda_k$ of a particular f-electron configuration w by filling in the lowest N_d one-electron levels. (iv) Generate a new configuration w' by moving a randomly chosen electron to a new position which is chosen also at random. (v) Calculate the ground-state energy $E(w')$. If $E(w') < E(w)$ the new configuration is accepted, otherwise w' is rejected. Then the steps (ii)-(v) are repeated until the convergence (for given parameters of the model) is reached. Of course, one can move instead of one electron (in step (iv)) simultaneously two or more electrons, thereby the convergence of the method is improved. Indeed, tests that we have performed for a wide range of the model parameters showed that the latter implementation of the method, in which $1 < p < p_{max}$ electrons (p should be chosen at random) are moved to
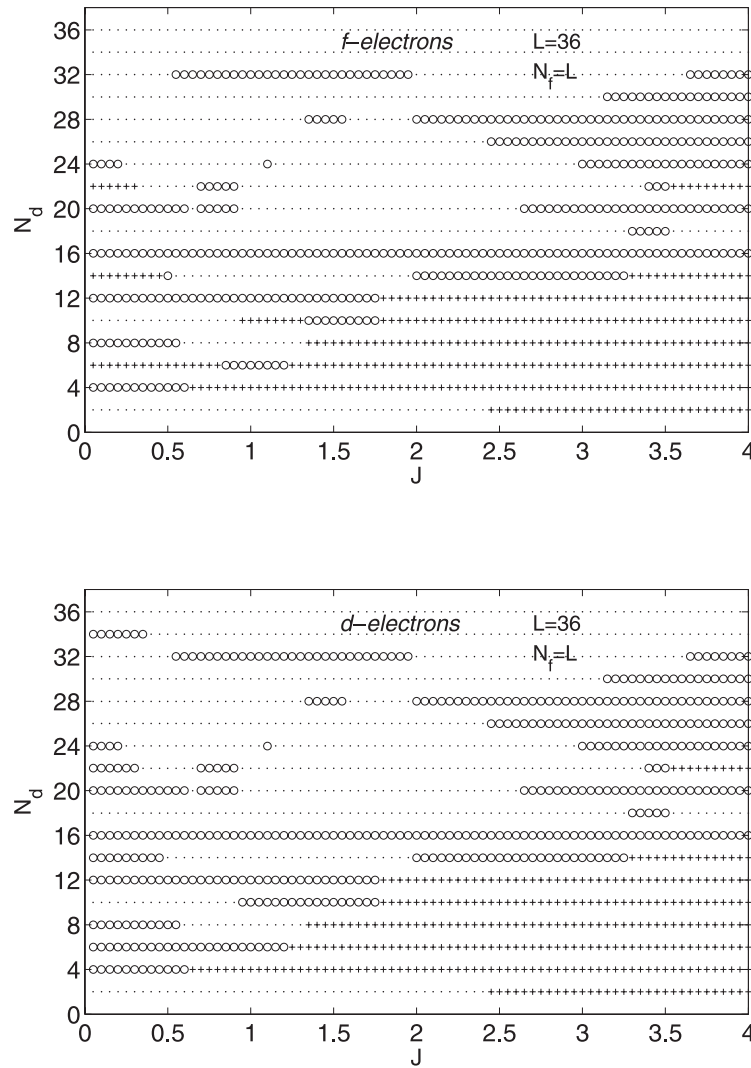
Fig. 4. The f and d electron phase diagrams of the spin-one-half FKM extended by the spin-dependent interaction calculated for $N_f < L, J = 0.5$ and $L = 48$. ($\cdot$): the NP phase, ($+$): the FP phase, ($\circ$): the PP phase. The one-dimensional approximative results.

new positions overcomes better the local minima of the ground state energy. In this paper we perform calculations with $p_{max} = N_f$. The main advantage of this implementation is that in any iteration step the system has a chance to lower its energy (even if it is in a local minimum), thereby the problem of local minima is strongly reduced (in principle, the method becomes exact if the number of iteration steps goes to infinity). On the other hand a disadvantage of this selection is that the method converges slower than for $p_{max} = 2$ and $p_{max} = 3$. To speed up the convergence of the method (for $p_{max} = N_f$) and still to hold its advantage we generate instead the random number p (in step (iv)), the pseudo-random number p that probability of choosing decreases (according to the power law) with increasing p (the larger a value of p the smaller probability of its choosing). Such a modification improves considerably the convergence of the method.

To test the convergence of the method we have first calculated the ground-state configurations of the model in the $N_f - N_d$ plane on the cluster of $L = 24$ sites. Comparing these results with exact ones (discussed above) we

have found that the method is able to reproduce the exact ground states after relatively small number of iterations (typically 5000–10 000 iterations per site). Then we have used the method to study the $N_f - N_d$ phase diagram of the model on larger clusters consisting of $L = 36$ and $L = 48$ sites. Our numerical computations showed that all main results obtained on small clusters hold also on larger clusters. Again we have observed strong coupling between f and d electron subsystems and a coincidence of corresponding magnetic phases, that stability regions are practically unchanged with increasing L (see Fig. 4). Moreover, we have observed that the main configurations types found for $L = 24$ persist also on large clusters and thus we suppose that the real magnetic phase diagram of the model will be very close to ones presented in Figures 3 and 4, Of course, it is possible that some ground states that are uniform on the finite lattices could be degenerated in the thermodynamic limit.

The same calculations we have performed also in two dimensions. The two-dimensional results are of particular importance since they could shed light on the mechanism
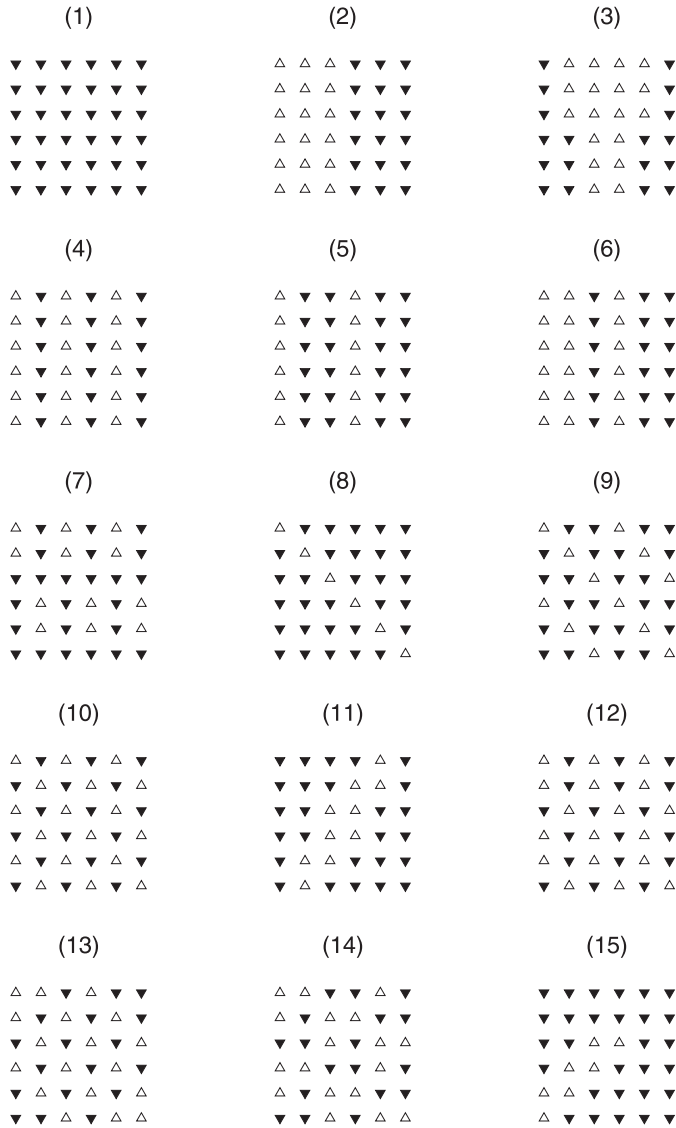
Fig. 5. The f and d electron ground-state phase diagrams of the spin-one-half FKM extended by the spin-dependent interaction calculated for $N_f = L$ ($L = 36$). The two-dimensional approximative results.

of two-dimensional charge and magnetic ordering in doped nickelate [1] and cuprate [2] materials. Here we concern our attention on a description of basic types of charge and magnetic ordering that exhibits the spin-one-half FKM with spin-dependent interaction between d and f electrons in two dimensions. To minimize the finite-size effects the numerical calculations have been done on three different clusters of 4×4, 6×6 and 8×8 sites. On the 4×4 cluster the calculations were performed by exact-diagonalization method and on larger clusters the approximative method described above was used.

Similarly as in the one dimension we start our two-dimensional studies with the case $N_f = L$. The magnetic phase diagrams of the f and d electron subsystems calculated for $N_f = L$ ($L = 36$) are shown in Figure 5. Comparing these phase diagrams with their one-dimensional counterparts one can find obvious similarities. In both cases the basic structure of the phase diagram is formed by three large FP, PP and NP domains that are accom-

panied by secondary phases (points in which the d and f electron phase diagrams do not coincide). However, while in the one dimension the secondary phases are stable only in isolated points at very small values of J, in two dimensions these secondary phases persist also for large J. Calculations that we have performed on different clusters (4×4, 6×6, and 8×8) showed that the secondary structure depends very strongly on the cluster-size (with increasing L it is gradually suppressed) and it is not excluded that it fully disappears in the thermodynamic limit ($L \to \infty$).

The typical examples of the ground-state configurations (that represent the most frequently appearing types of the ground states in the $N_d - J$ phase diagram) are displayed in Figure 6. Again one can see that the spectrum of magnetic solutions that yields the FKM extended by spin-dependent interaction is very rich. In addition to the FP phase (that the stability region shifts to higher d-electron concentrations when J increases) there are various types of NP and PP structures like the antiparallel ferromagnetic

Fig. 6. Typical examples of ground states of the spin-one-half FKM extended by the spin-dependent interaction obtained for $N_f = L$ ($L = 36$). To visualize the spin distributions we use $\triangle$ for the up spin electrons and $\triangledown$ for the down spin electrons. The two-dimensional approximative results.

domains (2–3), the axial magnetic stripes (4–7), the diagonal magnetic stripes (8–11) and the perturbed diagonal magnetic stripes (12–15). This again demonstrates strong effects of the spin-dependent interaction on the formation of magnetic superstructures in the extended FKM and its importance for a correct description of correlated electron systems.

From the experimental point of view the most interesting case is, however, the case $N_f < L$ that could model the real situation in doped nickelate and cuprate systems [1,2]. To describe possible charge and magnetic orderings for $N_f < L$ we have performed exhaustive studies of the

model on the 6×6 and 8×8 clusters. Numerical calculations have been done over the full set of N_f and N_d values and they revealed a rich spectrum of coexisting charge and magnetic superstructures. Some typical examples of these superstructures are presented in Figure 7. Between them one can find various types of phase segregated (e.g., 1), phase separated (e.g., 16) and n-molecular (e.g., 3) configurations with FP, PP and NP ground states as well as various types of axial (e.g., 9) and diagonal (e.g., 5) magnetic/charge stripes. Just the observation of phase segregation and phase separation is the main difference between our and Lemanski's results [5]. The latter were obtained only on the restricted set of periodic configurations and therefore they were not able to describe these important phenomena. In generally, we have observed that the system has tendency towards the phase segregation for small and large d-electron concentrations, while near the $n_d = 1$ point the system prefers to form the various types of axial and diagonal stripes. In addition, similarly as in $D = 1$ a strong reduction of FP and PP phases with decreasing N_f is observed also in $D = 2$. We have found that the same tendencies and the same types of configurations persist on both examined lattices (6×6 and 8×8), confirming the stability of obtained results.

Although we have presented here only the basic types of charge and magnetic superstructures (a more complete set will be given elsewhere) they clearly demonstrate an ability of the model to describe different types of charge and magnetic ordering. This opens an alternative route for understanding of formation an inhomogeneous charge/magnetic order in strongly correlated electron systems. In comparison to previous studies of this phenomenon based on the Hubbard and $t - J$ model [9], the study within the generalized spin-one-half FKM has one essential advantage and namely that it can be performed in a controllable way (due to the condition $[f_{i\sigma}^+ f_{i\sigma}, H] = 0$), and in addition it allows easily to incorporate and examine effects of various factors (e.g., an external magnetic field, nonlocal interactions, etc.) on formation of charge and magnetic superstructures. The work in this direction is currently in progress.

In summary, a combination of small-cluster exact-diagonalization calculations and a well-controlled approximative method was used to study the ground-state phase diagrams of the generalized spin-1/2 FKM with an anisotropic, spin-dependent on-site interaction between localized and itinerant electrons for $N_f = L$ ($0 \leq J \leq 1$ in $D = 1$ and $0 \leq J \leq 4$ in $D = 2$) and $N_f < L$ ($J = 0.5$). For both cases it was observed that the anisotropic, spin-dependent interaction induces strong coupling between the localized and itinerant subsystems and that the magnetic phase diagrams of these subsystems coincide. In general, the spin-dependent interaction (for $N_f = L$) stabilizes the FP and PP state, while the stability region of NP phase is gradually reduced. The opposite effect on the FP, PP and NP phases has a reduction of N_f. For both $N_f = L$ and $N_f < L$ an extremely rich spectrum of charge and magnetic solutions has been found. In particular, we have observed various types of phase segregated, phase
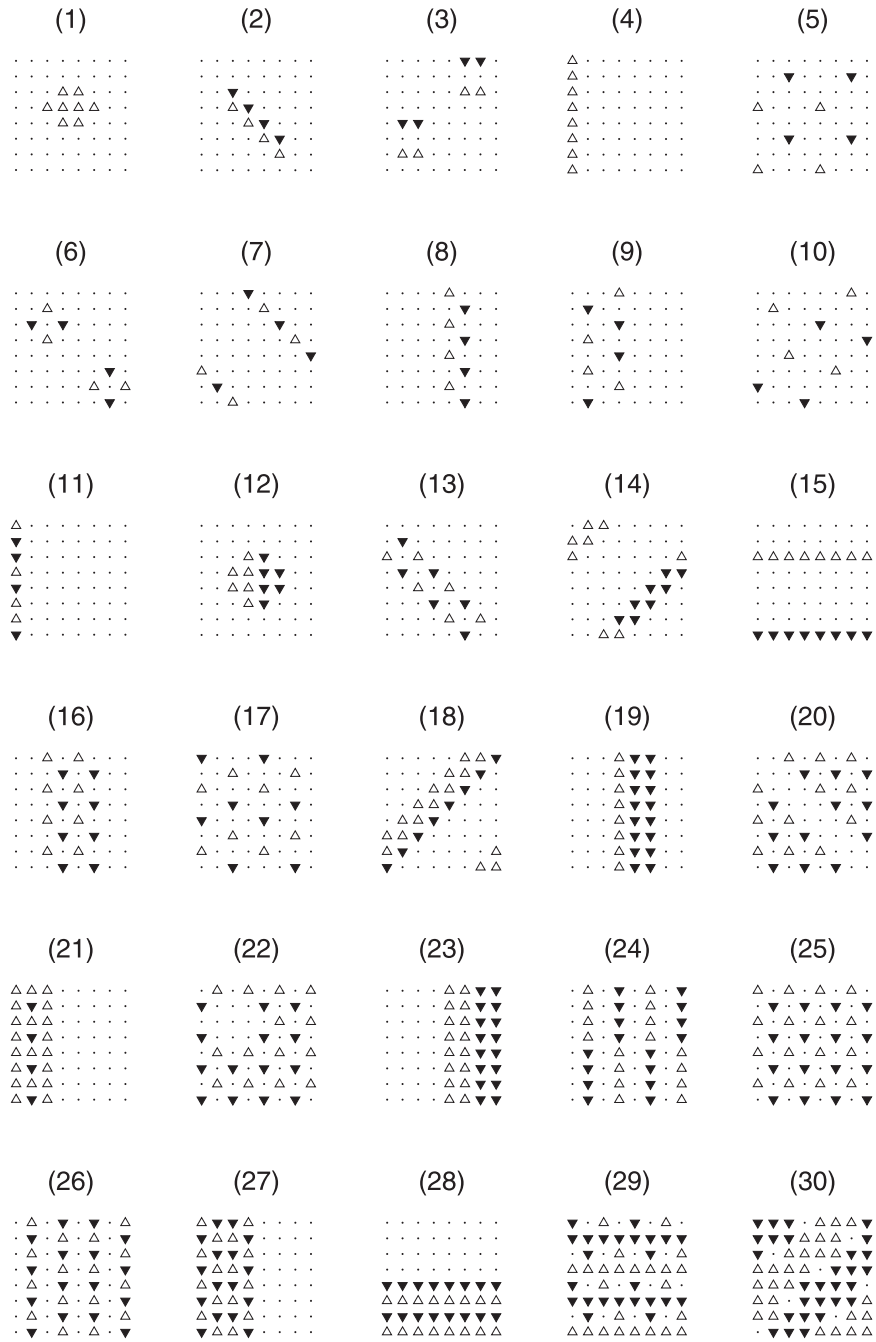
Fig. 7. Typical examples of ground states of the spin-one-half FKM extended by the spin-dependent interaction obtained for $N_f < L, J = 0.5$ and $L = 64$. The two-dimensional approximative results.

separated, striped, periodic and non periodic charge/spin distributions that clearly demonstrate strong cooperative effects of spin-dependent interaction on the ground states of the model.

References

1. C.H. Chen, S.-W. Cheong, A.S. Cooper, Phys. Rev. Lett. **71**, 2461 (1993); J.M. Tranquada, D.J. Buttrey, V. Sachan, J.E. Lorenzo, Phys. Rev. Lett. **73**, 1003 (1994); J.M. Tranquada, D.J. Buttrey, V. Sachan, J.E. Lorenzo,

Phys. Rev. B **52**, 3581 (1995); V. Sachan et al., Phys. Rev. B **51**, 12742 (1995)

2. J.M. Tranquada, B.J. Sternlieb, J.D. Axe, Y. Nakamura, S. Uchida, Nature (London) **375**, 561 (1995); J.M. Tranquada, B.J. Sternlieb, J.D. Axe, Y. Nakamura, S. Uchida, Phys. Rev. B **54**, 7489 (1996); J.M. Tranquada, B.J. Sternlieb, J.D. Axe, Y. Nakamura, S. Uchida, Phys. Rev. Lett. **78**, 338 (1997); H.A. Mook, P. Dai, F. Dogan, Phys. Rev. Lett. **88**, 097004 (2002)

3. L.M. Falicov, J.C. Kimball, Phys. Rev. Lett. **22**, 997 (1969)

4. R. Lemanski, J.K. Freericks, G. Banach, Phys. Rev. Lett. **89**, 196403 (2002)

5. R. Lemanski, Phys. Rev. B **71**, 035107 (2005)

6. E. Dagotto, Rev. Mod. Phys. **66**, 763 (1994)

7. P. Farkašovský, Eur. Phys. J. B **20**, 209 (2001)

8. H. Čenčariková, P. Farkašovský, Int. J. Mod. Phys. B **18**, 357 (2004)

9. V.J. Emery, S.A. Kivelson, H.Q. Lin, Phys. Rev. Lett. **64**, 475 (1990); L.P. Pryadko, S.A. Kivelson, D.W. Hone, Phys. Rev. Lett. **80**, 5651 (1998); S.R. White, D.J. Scalapino, Phys. Rev. Lett. **80**, 1272 (1998); S.R. White, D.J. Scalapino, Phys. Rev. Lett. **81**, 3227 (1998); S.R. White, D.J. Scalapino, Phys. Rev. B **60**, R753 (1999); S.R. White, D.J. Scalapino, Phys. Rev. B **61**, 6320 (2000); A.M. Oles, Acta Physica Polonica B **31**, 2963 (2000); J. Frolich, D. Uettschi, J. Stat. Phys. **118**, 973 (2005)